Monte Carlo Simulations of Defect-Free Cross-Linked Gels in the Presence of Salt

ARTICLE *in* MACROMOLECULES · NOVEMBER 2004

Impact Factor: 5.8 · DOI: 10.1021/ma0486391

3 AUTHORS, INCLUDING:

Stefanie Schneider
RWTH Aachen University
13 PUBLICATIONS **354** CITATIONS

Monte Carlo Simulations of Defect-Free Cross-Linked Gels in the Presence of Salt

Samuel Edgecombe,* Stefanie Schneider, and Per Linse

Physical Chemistry 1, Centre for Chemistry and Chemical Engineering, Lund University, P.O. Box 124, S-22100 Lund, Sweden

Received July 6, 2004; Revised Manuscript Received September 13, 2004

ABSTRACT: Properties of polyelectrolyte gels in equilibrium with a reservoir of salt solution described within the primitive model have been investigated using Monte Carlo simulations. The polyelectrolyte gel was modeled as a charged defect-free three-dimensional network of diamondlike topology with explicit simple ions. The deswelling upon addition of salt was investigated for gels with different charge density, cross-linking density, chain flexibility, and counterion valence. All polyelectrolyte gels underwent a deswelling upon addition of salt. In most systems, however, even at high salt concentration, the equilibrium volumes remained significantly larger than those of the corresponding uncharged gels, and the salt concentration in the gel remained smaller than that in the reservoir. The salt content in the gel was larger as compared to that predicted by an ideal Donnan equilibrium due to a more negative excess chemical potential of the salt in the gel as compared to that in the reservoir. The predictions of the Flory−Rehner−Donnan theory were qualitatively in agreement with our results, but they displayed significant quantitative disagreement, mainly due to an overestimated contribution from the counterions to the osmotic pressure.

1. Introduction

Chemically cross-linked polymer and polyelectrolyte gels have been of great interest for more than half a century.[1] Such gels possess unique elastic properties of vital technological use and are still of strong scientific interest. The properties of a swollen network depend on a number of factors including the selection of monomers, ratio of monomer to cross-linker, solvent quality, and synthesis protocol. For polyelectrolytes, the salt content and the pH (if the polyelectrolyte gel possesses titratable groups) are of use when controlling the gel volume. Swollen polyelectrolyte gels, often referred to as hydrogels, are used, for example, in hygiene products such as diapers, in pharmaceutical products such as drug deliverers, and in the agriculture sector as moisture retainers.

Experimental studies have shown that in the absence of salt, polyelectrolyte gels in water are often highly swollen.[1] Upon addition of salt, the degree of swelling decreases and sometimes a sharp volume reduction appears over a narrow salt concentration range.[2−5] Ohimine and Tanaka showed that salt containing divalent counterions reduced the gel volume much more efficiently than salt containing monovalent counterions.[3]

It is a challenge to describe the swelling of polyelectrolyte gels, since the equilibrium swelling arises from a delicate balance of several factors. In most of the common approaches, an expression of the difference in the osmotic pressure in the gel and the surrounding solution is employed. Typically, such pressure differences include terms describing (i) the network elasticity with expressions dating back to the earliest molecular based theories of polymer networks by Flory and Rehner[6,7] and Wall[8] (affine model) and from James and Guth[9] (phantom model), (ii) the enthalpic contribution from the polymer−solvent interaction from Flory,[10] and (iii) the osmotic pressure originating from the simple ions using ideal conditions and a Donnan equilibrium.[11,12] Some of the theoretical approaches were reviewed by Khokhlov.[13] Despite the simplicity of these models, qualitative, and sometimes near quantitative, agreement with experiments is often quoted. However, with divalent counterions less satisfactory agreement was reported by Ricka and Tanaka.[4] Okay and Sariisik[5] needed an effective network charge density to obtain a satisfactory description. These two examples suggest that an improved treatment of the electrostatic interaction is needed.

Monte Carlo simulations and molecular dynamics are two indispensable tools to obtain properties of molecular systems. Over the past few decades, they have been applied to examine, e.g., properties of simple liquids,[14] polymers and polymer solutions,[15] solutions of biomolecules, and self-association and association in colloidal science. Comparably lately, these techniques have been applied to cross-linked polymer gels; e.g., see the review by Escobedo and de Pablo.[16]

Recently, in our laboratory we have performed Monte Carlo simulations of polyelectrolyte gels based on the primitive model of electrolytes, which is a well-established approach for describing electrolyte solutions. Properties of cross-linked polyelectrolyte gels with idealized network topology in equilibrium with a pure solvent reservoir have been investigated.[17−19] In particular, the origin of the large swelling capacity,[17] how the swelling depends on parameters describing the gel,[18] and the appearance of discontinuous volume transitions[19] have been addressed. These studies also showed that the Gaussian chain approximation and the affine approximation, applied in nearly all theories, are questionable simplifications and may not be at all applicable in some cases. Yan and de Pablo have also performed similar simulations using the primitive model and examined the gel swelling as a function of the Bjerrum length (the electrostatic coupling),[20] whereas Lu and Hentschke have used a different model containing explicit solvent molecules.[21]

* To whom correspondence should be sent. E-mail: samuel.edgecombe@fkem1.lu.se.

10.1021/ma0486391 CCC: $27.50
Published on Web 11/24/2004

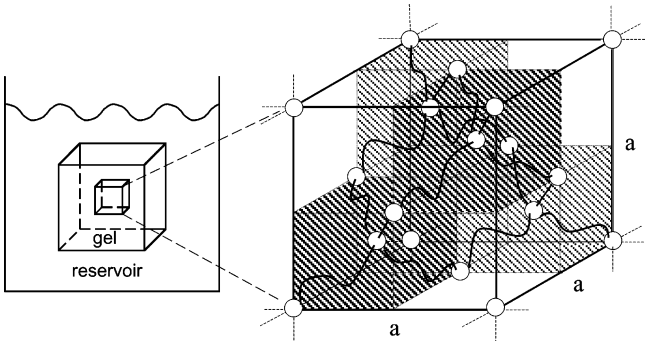

Figure 1. Left: Schematic illustration of a cubic macroscopic gel in a reservoir of solvent. Right: Schematic illustration of one unit cell of a defect-free network of diamondlike topology containing eight tetra-functional nodes (spheres) linked by noncrossing chains (wavy lines). Note that four of the eight subcubes contain chains (shaded), whereas the other four are empty.

In this communication, we extend our investigations of cross-linked polyelectrolyte gels to include the case of the gel being in equilibrium with a reservoir containing a simple salt, again using the primitive model. At such conditions, the theoretical framework becomes more complex. Now equilibrium requires equal pressure *and* equal chemical potential of the salt in the gel phase and the reservoir, whereas in the previous investigations without salt only the equal pressure condition was required. Not unexpectedly, our results show that the polyelectrolyte gel contracts as the salt concentration in the reservoir is increased. However, the response depends substantially on the properties of the network and on the counterion valence. We also examine the ideal and nonideal Donnan equilibrium in some detail and find that the nonideality increases the salt content in the polyelectrolyte gel. Finally, we compare the Flory–Rehner theory with our results and show that this theory is able to qualitatively, but not quantitatively, describe the simulated swelling data.

2. Model

The polyelectrolyte gel with added simple salt is described within the primitive model. The same approach as in the previous articles by Schneider and Linse[17–19] is used.

To simplify our description, the anion of the salt is identical to the counterion of the charged network and they are collectively referred to as counterions. Our system of interest, thus, contains a charged network, counterions and co-ions, and implicit solvent. All charged species are treated explicitly as charged hard spheres, whereas the solvent is modeled as a dielectric continuum. The network is composed of chains connected by tetra-functional charged cross-linkers (nodes). Each chain is modeled as a sequence of charged hard spheres (beads), which are connected by harmonic bonds. A defect-free network of diamondlike topology is used, in which all the chains are of equal length. The chains are not allowed to cross each other; thus, the topology of the network remains fixed, and the model represents a covalently cross-linked network (see Figure 1, right).

The gel is composed of a network containing N_{node} nodes and N_{chain} chains, $N_{\text{counterion}}$ unconnected charged counterions, and $N_{\text{co-ion}}$ unconnected charged co-ions. Each chain is composed of n_{bead} beads. Hence, there are in total $N = N_{\text{network}} + N_{\text{counterion}} + N_{\text{co-ion}}$ particles, where the number of network particles is $N_{\text{network}} = N_{\text{node}} + N_{\text{chain}} n_{\text{bead}}$. Electroneutrality is assured by suitable choice of $N_{\text{counterion}}$ and $N_{\text{co-ion}}$.

The total potential energy, U, of a system can be expressed as the sum of a nonbonded potential energy (Coulomb interaction plus hard-core repulsion), U_{nonbond}, a bond potential energy, U_{bond}, and an angular potential energy, U_{angle}, according to

$$U = U_{\text{nonbond}} + U_{\text{bond}} + U_{\text{angle}} \tag{1}$$

The nonbonded potential energy is taken to be pairwise additive according to $U_{\text{nonbond}} = \sum_{i<j} u_{ij}(r_{ij})$. The pair potential u_{ij} for pair ij, where i and j denote either a node, a bead, a counterion, or a co-ion, is given by

$$u_{ij}(r_{ij}) = \begin{cases} \infty & r_{ij} < R_i + R_j \\ \dfrac{z_i z_j e^2}{4\pi\epsilon_0\epsilon_r r_{ij}} & r_{ij} \geq R_i + R_j \end{cases} \tag{2}$$

where z_i is the charge of particle i, R_i the radius of particle i, e the elementary charge, ϵ_0 the dielectric permittivity in a vacuum, ϵ_r the relative permittivity of the solvent, and $r_{ij} = |\mathbf{r}_{ij}| = |\mathbf{r}_i - \mathbf{r}_j|$ the distance between the centers of particles i and j. The bond potential energy is given by

$$U_{\text{bond}} = \sum_{m=1}^{N_{\text{bond}}} \frac{k_{\text{bond}}}{2}(r_{m,\text{bond}} - r_0)^2 \tag{3}$$

where N_{bond} is the number of bonds in the network, $r_{m,\text{bond}}$ the bond length, $r_0 = 0.5$ nm the unperturbed equilibrium distance, and $k_{\text{bond}} = 0.4$ N/m the spring constant. Taking into account all interactions in the system, the typical root-mean-square separation between bonded beads becomes $\approx$0.55–0.60 nm. The angular potential energy is given by

$$U_{\text{angle}} = \sum_{m=1}^{N_{\text{chain}}} \sum_{i=2}^{n_{\text{bead}}} \frac{k_{\text{angle}}}{2}(\alpha_{i\in m} - \alpha_0)^2 \tag{4}$$

where N_{chain} is the number of polymer chains, n_{bead} the number of beads per chain, $\alpha_{i\in m}$ the bond angle formed by three consecutive beads in chain m with bead i as the central bead, k_{angle} the force constant, and $\alpha_0 = 180°$ the unperturbed equilibrium angle. The bare persistence length, characterizing the intrinsic stiffness of the chain, was determined in separate simulations of the corresponding linear uncharged chains.[22]

Five polyelectrolyte gels have been examined at different salt conditions. The reference system is characterized by $z_{\text{node}} = z_{\text{bead}} = 1$, $n_{\text{bead}} = 20$, $k_{\text{angle}} = 0$, and $z_{\text{counterion}} = -1$. To study the effect of changing one single parameter, four systems identical to the reference system except for the value of one parameter have been considered. System I contains network particles with a reduced net charge ($z_{\text{node}} = z_{\text{bead}} = 0.5$), system II has shorter chains ($n_{\text{bead}} = 10$), system III has stiffer chains ($k_{\text{angle}} = 8.3 \times 10^{-23}$ J deg^{-2} resulting in the bare persistence length $l_p = 37$ nm), and system IV has divalent counterions ($z_{\text{counterion}} = -2$). In all systems, particle radius $R_i = R = 0.2$ nm, $T = 298$ K, and $\epsilon_r = 80$ have been used. General data of the model are given in Table 1, whereas data specific for the individual systems are provided in Table 2. All systems have earlier been studied in the salt-free limit.[18] In addition, volumes of the corresponding uncharged networks without simple

Table 1. General Data for the Model

box length	$L = 9-25$ nm
node radius	$R_{node} = 0.2$ nm
bead radius	$R_{bead} = 0.2$ nm
counterion radius	$R_{counterion} = 0.2$ nm
co-ion radius	$R_{co-ion} = 0.2$ nm
node charge	$z_{node} = +1/2$ and $+1$
bead charge	$z_{bead} = +1/2$ and $+1$
counterion charge	$z_{counterion} = -1$ and -2
co-ion charge	$z_{co-ion} = +1$
chain persistence length	$l_p = 0.7$ and 37 nm
fraction of nodes	$x_{node} = 0.025$ and 0.050
no. of beads per chain	$n_{bead} = 10$ and 20
temperature	$T = 298$
relative permittivity	$\epsilon_r = 80.0$

Table 2. Specific Data for Different Polyelectrolyte Gel Systems

gel system	$z_{node} = z_{bead}$	n_{bead}	k_{angle} (10^{-23} J deg^{-2})	$z_{counterion}$
ref system	+1.0	20	0.0	−1.0
system I	+0.5	20	0.0	−1.0
system II	+1.0	10	0.0	−1.0
system III	+1.0	20	8.3	−1.0
system IV	+1.0	20	0.0	−2.0

ions and in equilibrium with a salt-free reservoir have been determined.

The polyelectrolyte gel is regarded to be in contact with a reservoir containing simple salt with an exchange of solvent and salt between the gel and the reservoir (see Figure 1, left). An equilibrium swelling of the gel is reached when (i) the osmotic pressures in the gel P and in the reservoir P^{res} are equal and (ii) the chemical potentials of the salt in the gel μ and in the reservoir μ^{res} are equal according to

$$P = P^{res} \tag{5}$$

$$\mu = \mu^{res} \tag{6}$$

The chemical potential of the salt is given by

$$\mu = \nu_-\mu_- + \nu_+\mu_+ \tag{7}$$

where ν_- and ν_+ are the stoichiometric factors of the salt. In this study, we have $\nu_- = \nu_+ = 1$ for $z_{counterion} = -1$ and $z_{co-ion} = +1$ and $2\nu_- = \nu_+ = 2$ for $z_{counterion} = -2$ and $z_{co-ion} = +1$. The chemical potential of an individual ionic species μ_i is given by the sum of an ideal and an excess part according to

$$\mu_i = \ln(c_i) + \mu_i^{ex} \tag{8}$$

where c_i is the concentration and μ_i^{ex} the excess chemical potential of species i. The chemical potentials of the individual ionic species become

$$\mu_- = \ln(c_- + c_-^{salt}) + \mu_-^{ex} \tag{9a}$$

$$\mu_+ = \ln(c_+^{salt}) + \mu_+^{ex} \tag{9b}$$

in the gel and

$$\mu_-^{res} = \ln(c_-^{salt,res}) + \mu_-^{ex,res} \tag{10a}$$

$$\mu_+^{res} = \ln(c_+^{salt,res}) + \mu_+^{ex,res} \tag{10b}$$

in the reservoir. In eq 9a, c_- is the concentration of the counterions compensating the charge of the network. In eqs 9a and 9b, $c_i^{salt} = \nu_i c^{salt}$ with c^{salt} denoting the stoichiometric salt concentration in the gel, and in parts a and b of eq 10, $c_i^{salt,res} = \nu c_i^{salt,res}$ with $c^{salt,res}$ denoting the stoichiometric salt concentration in the reservoir. Note, in general $c^{salt} \neq c^{salt,res}$.

3.Method

3.1. Simulation Details. All particles were enclosed in a cubic box subjected to periodic boundary conditions. The Metropolis Monte Carlo (MC) protocol was used to generate Boltzmann-weighted configurations of the gel systems.[23] Both the canonical (*NVT*) ensemble (characterized by constant number of particles, volume, and temperature) and the isothermal−isobaric (*NPT*) ensemble (constant number of particles, pressure, and temperature) were employed.[14] The potential energies were calculated according to eqs 1−4, and the long-range electrostatic interactions were handled using the Ewald summation.[18,24,25] Unless otherwise stated, simulated systems comprised one unit cell containing $N_{node} = 8$ nodes and $N_{chain} = 16$ chains. A previous study[18] showed that the pressure of such systems had essentially converged with respect to the system size.

Initial configurations were generated by placing the nodes on a diamond lattice, and thereafter the nodes were connected by nonentangling chains. Counterions and co-ions were placed randomly. In the Metropolis algorithm, single particles were subjected to translational displacements ranging from 0.25 to 5.0 mm, smallest for the nodes and beads. Equilibration involved 10^4-10^5 trial moves per particle, and the production runs up to 2.5×10^5 trial moves per particle. In the *NPT*-MC simulations, an attempt to change the volume was made after $\approx N$ single-particle moves with an attempted volume change varying from 10 to 80 nm^3.

In addition to the simulations of the gel systems, Metropolis MC simulations of pure salt solutions in the *NVT* ensemble were performed to determine the osmotic pressure and the chemical potential of the salt as a function of the salt concentration. In total, 216 and 324 particles were used for the 1:1 and the 2:1 electrolyte solution, respectively. As before, a cubic box with periodic boundary conditions and the Ewald summation were used. The production runs involved 10^4 trial moves per particle.

The reported statistical uncertainty is given as one standard deviation of the mean estimated by dividing a simulation into 10−25 sub-batches. All simulations were performed using the integrated Monte Carlo/molecular dynamics/Brownian dynamics simulation package, MOLSIM.[26]

3.2. Pressure Evaluation. The (osmotic) pressure of a system with central and pairwise additive potentials can be expressed as the sum of the ideal pressure, a virial term, and a contact term (known as the virial route)[14] according to

$$P = P_{ideal} + P_{virial} + P_{contact} \tag{11}$$

where $P_{ideal} = ck_BT$ and $c = N/V$ with V being the volume of the system and N the total number of particles in the system and k_B the Boltzmann constant. The virial contribution becomes

$$P_{virial} = \frac{1}{3V}\left\langle \sum_i \sum_{j>i} \mathbf{r}_{ij} \cdot \mathbf{f}_{ij} \right\rangle \tag{12}$$

where $\mathbf{f}_{ij}$ is the force acting between particles i and j. The contact term arises from the infinite potential at hard-sphere contact and is given by

$$P_{contact} = \frac{2\pi}{3} k_B T \sum_i \sum_j (R_i + R_j)^3 c_i c_j g_{ij}(R_i + R_j) \tag{13}$$

where $c_i = N_i/V$ is the number density of particle type i and $g_{ij}(R_i + R_j)$ the value of the radial distribution function (rdf) between pair ij at contact separation $r_{ij} = R_i + R_j$. The contribution from the angular potential to the pressure is equal to zero. After adaptation to the Ewald formalism,[27] eqs 11−13 were used for the pressure evaluation.

3.3. Chemical Potential Evaluation. According to eq 8, the chemical potential of a species is given as the sum of an ideal and an excess part. Throughout, the ideal part was evaluated by expressing the number density in millimolar units. The excess part was determined by applying Widom's particle insertion method[28] using the minimum image (MI) convention for the energy evaluation. The particle insertion method is an efficient and nondisturbing method applicable to systems that are not too dense. The considerable system size dependence of the excess chemical potential of single ionic species can be avoided by using a coupling integration or by calculating the excess chemical potential of the salt by simultaneous multiple insertions.[29] Both approaches were applied, and they provided equal statistical results. Typically, 10^4 trial insertions were made after every 100 trial moves per particle.

The choice of the MI convention for calculating the excess chemical potential through Widom's method was governed by its simple implementation. Results of test simulations with the Ewald summation for the actual simulation replaced by the MI convention provided excess chemical potentials that deviated at most $0.05k_BT$ from the original protocol. Hence, we conclude that the present approach to obtain excess chemical potentials is satisfactory.

3.4. Establishment of Gel—Reservoir Equilibrium. As previously stated, our aim is to calculate properties of polyelectrolyte gels in equilibrium with a reservoir of known salt concentrations. Such equilibria were numerically determined by finding intersection points of the functions $P(\mu)$ and $P^{res}(\mu^{res})$. After the determination of the intersection points, where eqs 5 and 6 are satisfied, the salt concentrations in the gel c^{salt} and in the reservoir $c^{salt,res}$ can be determined. From the equilibrium volume V_{eq} and the number of particles of different types, other concentration variables than c^{salt} are readily available.

The function $P(\mu)$ for the gel was determined numerically. The reduced excess pressure and the reduced excess chemical potential of the salt as a function of the salt concentration were determined from MC simulations. By adding the ideal contributions, the functions $P(c^{salt})$ and $\mu(c^{salt})$ were obtained, and finally the function $P(\mu)$ with c^{salt} as an implicit parameter was constructed. Initially, simulations using both the *NVT* and the *NPT* ensemble were performed. The use of the *NPT* ensemble was found to be more favorable, since the intersecting angle of $P(\mu)$ and $P^{res}(\mu^{res})$ becomes larger, making the determination of the equilibrium pressures and chemical potentials and hence the equilibrium salt concentrations more accurate.

In a similar manner, the corresponding function $P^{res}(\mu^{res})$ for the reservoir with $c^{salt,res}$ as an implicit parameter was determined. Figure 2 shows the reduced excess pressure and the reduced excess chemical potential of the salt as a function of the salt concentration for a simple 1:1 and a 1:2 electrolyte determined from *NVT*-MC simulations (filled symbols connected with solid curves). The decrease of the excess pressure and the excess chemical potential at small and intermediate salt concentrations is due to the cohesiveness of the Coulomb interaction, whereas the increase at high salt concentrations arises from the hard-sphere part of the potential. Figure 2 also displays the corresponding data as predicted by the Debye–Hückel (DH) theory and the extended DH (EDH) theory.[30] The DH theory, which is exact in the limit $c^{salt,res} \to 0$, is accurate up to ≈10 mM for the 1:1 electrolyte, but only to a few mM for the 1:2 electrolyte. The EDH theory is applicable to roughly twice as high salt concentrations as compared to the DH theory.

For each of the investigated five gel systems, three or four equilibrium conditions were determined. Figure 3 illustrates the determination of the equilibrium conditions for the reference system using results from the *NPT* simulations of the polyelectrolyte gel. The horizontal curves (open circles connected with solid lines) denote pressures and chemical potentials of the salt in the gel for different c^{salt}. Along such a curve, both the gel volume and the number of salt particles vary. Table 3 provides a summary of the equilibrium pressures and chemical potentials determined for the five gel systems considered.

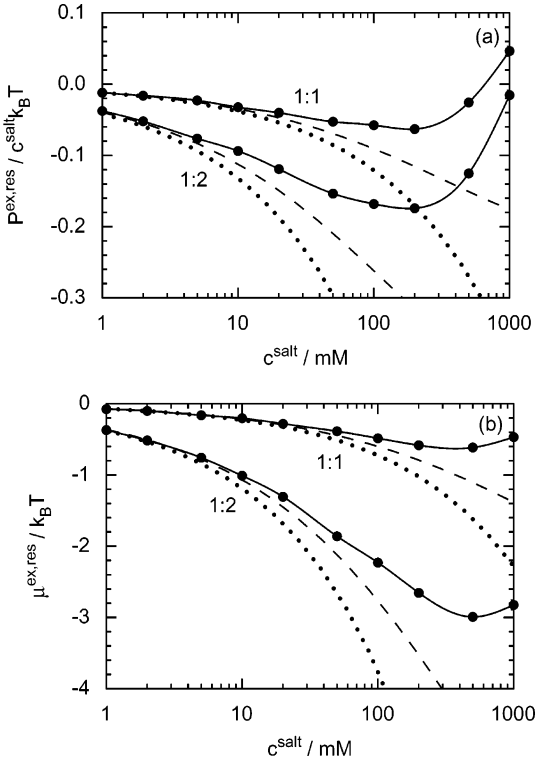

Figure 2. (a) Reduced excess pressure and (b) reduced excess chemical potential vs the salt concentration for a 1:1 electrolyte and a 1:2 electrolyte from *NVT* simulation (filled symbols connected by splines), the Debye–Hückel theory (dotted curves), and the extended Debye–Hückel theory (dashed curves). The uncertainties of the simulated data are approximately smaller than (c^{salt} < 1000 mM) or equal to (c^{salt} = 1000 mM) the size of the symbols.

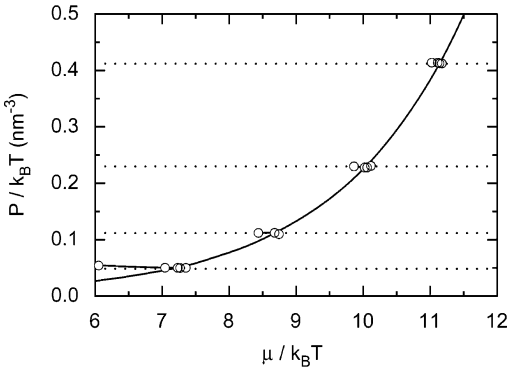

Figure 3. Pressure vs the reduced chemical potential of the salt for the reference system at four different external pressures from *NPT* simulations (open symbols connected by solid lines) and for the 1:1 electrolyte reservoir from *NVT* simulations (solid curve) using Widom's method. The external pressures, P_{ext}, of the *NPT* simulations are also given (dotted lines). See text for further details. The uncertainties in pressure and chemical potential are smaller than the size of the symbols.

4. Results and Discussion

4.1. Gel Deswelling. 4.1.1. Equilibrium Volume. Equilibrium volumes per network particle v_{eq} of the gels in equilibrium with a salt reservoir as a function of salt concentration in the reservoir $c^{salt,res}$ are shown in Figure 4a (symbols connected with solid lines). Corresponding numerical data are provided in Table 3. The volumes of corresponding uncharged networks without added salt in equilibrium with a salt-free reservoir are also given in Figure 4a (dotted lines). The networks of the reference system, system I, and system IV are identical;

Table 3. Selected Properties of the Gel and the Salt Reservoir at Equilibrium[a]

gel system	P_{ext}/k_BT[b] (nm^{-3})	P/k_BT[c] (nm^{-3})	μ/k_BT[d]	v_{eq}[e] (nm^3)	c^{salt}[f] (mM)	$c^{salt,res}$[g] (mM)
reference				25.9	0	0
	0.049	0.050(3)	7.233(4)	14.9	27.1	45.0
	0.112	0.112(3)	8.679(4)	9.01	62.9	96.9
	0.231	0.228(3)	10.023(4)	7.43	150	203
	0.413	0.413(1)	11.140(4)	5.96	279	358
system I				15.0	0	0
	0.292	0.292(1)	10.481(4)	3.49	174	255
	0.729	0.729(1)	12.227(6)	2.82	466	611
	1.094	1.098(3)	13.071(4)	2.78	710	884
system II				7.45	0	0
	0.243	0.245(1)	10.188(7)	3.90	127	219
	0.437	0.441(2)	11.256(6)	3.27	242	380
	0.875	0.885(1)	12.636(6)	2.98	530	724
system III				66.9	0	0
	0.0243	0.0244(1)	5.930(3)	59.6	17.0	22.6
	0.0729	0.0718(2)	7.869(2)	50.4	55.3	63.0
	0.1215	0.1219(4)	8.821(4)	49.8	96.5	105
system IV				3.34	0	0
	0.243	0.229(1)	14.0(1)	2.80	135.7	152.0
	0.486	0.483(1)	15.8(2)	2.71	280.7	321.0
	0.729	0.720(1)	16.8(1)	2.71	410.9	464.0

[a] Data of the gel systems investigated, which are located closest to the $P(\mu) - P^{res}(\mu^{res}) -$ intersection. The difference in the values of P and μ between these systems and at the intersections affects V_{eq} and the equilibrium salt concentrations only marginally. [b] External osmotic pressure in the *NPT* simulations. [c] Osmotic pressure according to eqs 11−13. [d] Chemical potential of the salt according to eqs 7−10. [e] Gel equilibrium volume per network particle, $v_{eq} = V_{eq}/N_{network}$. [f] Salt concentration in the gel. [g] Salt concentration in the reservoir.

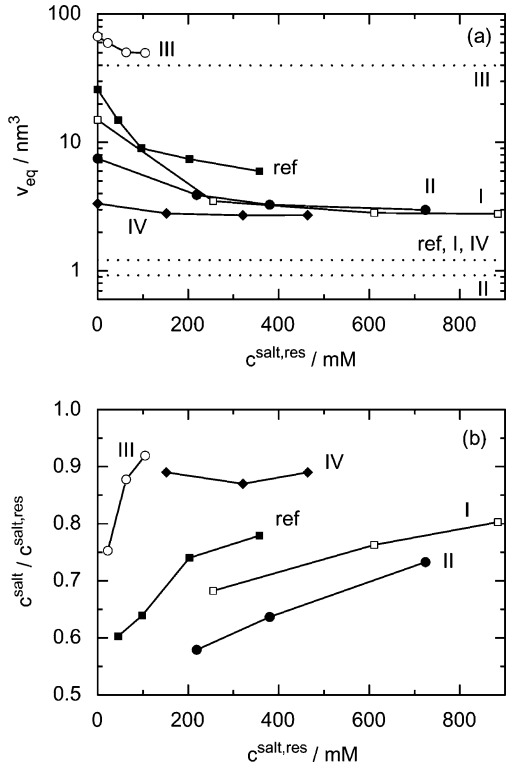

Figure 4. (a) Equilibrium volume per network particle and (b) ratio of the salt concentration in the gel and in the reservoir vs the salt concentration in the reservoir for indicated gel systems (symbols connected by solid lines). In part a, the volume per network particle of the corresponding uncharged networks without added salt in equilibrium with a salt-free reservoir is also shown (dotted lines).

thus, their uncharged equilibrium volumes also become identical.

In the salt-free limit, v_{eq} varies 20-fold for the different systems considered (symbols on the vertical axis in Figure 4a). As compared to the reference system, reducing linear charge density (system I), increasing the cross-linking density (system II), and increasing the valence of the counterion (system IV) all reduce the equilibrium volume per network particle. By increasing chain stiffness (system III), equilibrium swelling is increased. Among systems I, II, and IV, the volume reduction is smallest in system I and largest in system IV.

As the salt concentration in the reservoir is increased from the salt-free limit, the equilibrium volumes of the gels are reduced. This observation is in qualitative agreement with experimental observations.[2−5] So far, we have only encountered a gradual decrease of the gel volume at increasing salt concentration. In a previous study[19] it was concluded that the presence of a short-range attractive interaction or a stronger electrostatic interaction, e.g., by reducing the relative permittivity of the solvent, can lead to a discontinuous volume transition for the selected gel model. Possibly, a discontinuous transition at increasing salt concentration would appear if, e.g., a similar short-range attraction had been included.

Despite their identical networks, the deswelling characteristics of the reference system, system I, and system IV upon addition of salt are different (see Figure 4a). Regarding the reference system, at $c^{salt,res} = 360$ mM its original equilibrium volume is nearly 4-fold reduced, but is still 5-fold larger than the corresponding uncharged network without added salt. The gel with the reduced linear charge density (system I) displays throughout a smaller swelling than the reference system and approaches twice the volume of the uncharged network without added salt. With the monovalent counterions replaced by divalent ones (system IV), the equilibrium volume of the salt-free gel was, as mentioned, significantly smaller, and the volume is only marginally dependent upon addition of the 2:1 salt. At high reservoir salt concentration (≈500 mM) the equilibrium volume of system IV is roughly twice that of the corresponding uncharged network.

The gel with the higher cross-linking density (system II) also displays a smaller relative volume reduction as compared to the reference system. The shorter chains between the nodes reduce the ability of the gel to swell

in equilibrium with a salt-free reservoir, and the subsequent deswelling upon addition of salt hence becomes less pronounced. At high salt concentrations, the equilibrium volume is three times as large as that of its uncharged network.

The gel volume with the stiffest chains (system III) in equilibrium with a salt-free reservoir is only twice as large as that of its uncharged network. As salt is added, the gel deswells rapidly to the equilibrium volume of the corresponding uncharged network, but the relative volume change upon the salt addition is small. In this system, the bare persistence length of the chains is three times its contour length; hence the chains are near rigid rods (see also the snapshot of system IIIb in Table 2 of ref 18). The large gel volume is thus rather a consequence of the rigid chains than of an osmotic swelling, which is consistent with the relative small deswelling upon addition of salt.

To conclude, the gel systems considered display a rich behavior as salt is added. For a highly charged gel with unit charges separated 0.5−0.6 nm along the chain (the reference system), a considerable deswelling upon addition of salt appears, but the volume of the corresponding uncharged network without added salt is not reached. As the linear charge density is reduced (system I), the high-salt limit becomes closer to the charge-free one, but still not coinciding that even at near molar salt concentration. Making the chains shorter (system II), reduces the volume deswelling at large salt concentrations somewhat. With the stiff chain (system III), the deswelling is weak and occurs already at low salt content. Finally, with divalent counterions (system IV) the deswelling is very weak.

4.1.2. Salt Concentration in the Gels. The ratios of the salt concentration in the gel, c^{salt}, and in the reservoir, $c^{salt,res}$, as a function of the salt concentration in the reservoir are displayed in Figure 4b. Generally, and as expected, (i) the salt concentration in the gel is smaller than that in the reservoir ($c^{salt} < c^{salt,res}$) and (ii) the ratio of the salt concentration in the gel and in the reservoir increases as the salt concentration increases ($c^{salt}/c^{salt,res}$ grows with increasing $c^{salt,res}$). In most cases, the ratio $c^{salt}/c^{salt,res}$ is between 0.6 and 0.9.

Regarding the reference system, system I, and system II, at high high-salt concentrations the ratio $c^{salt}/c^{salt,res}$ is yet far from unity, which is related to the observation that the equilibrium volume did not reach the charge-free limit. The reason for $c^{salt}/c^{salt,res}$ still being smaller than unity at high $c^{salt,res}$ is the high concentration of charged network particles with a correspondingly large c_- (≈300 to 550 mM) (further discussed below). In the case of system III (stiffer chains), $c^{salt}/c^{salt,res}$ approaches unity at much lower $c^{salt,res}$, an effect of the much smaller network concentration and likewise small c_- (≈30 mM). Finally, for system IV with divalent counterions, $c^{salt}/c^{salt,res}$ takes practically the constant value 0.9 and is greater than the ratios for all other systems except system III. It appears consistent that the sensitivity of v_{eq} and $c^{salt}/c^{salt,res}$ on $c^{salt,res}$ is similar.

4.2. Donnan Equilibrium. We will now examine the Donnan equilibrium, i.e., the relation between the salt concentration in the gel c^{salt} and in the reservoir $c^{salt,res}$ in some detail. This will be made at two different conditions, viz. (i) nonzero excess chemical potential of the salt with gel volume $V_{(i)}$ (below referred to as the *nonideal* condition) and (ii) zero excess chemical potential of the salt, $\mu^{ex} \equiv \mu^{ex,res} \equiv 0$, (referred to as the *ideal* condition), of which we split the second one into two subconditions according to (ii.a) the ideal condition with the same gel volume as the nonideal one ($V_{(ii.a)} = V_{(i)}$) and hence no pressure equilibrium (referred to as the *unrelaxed* ideal condition) and (ii.b) the ideal condition with a different gel volume ($V_{(ii.b)} \neq V_{(i)}$) such that pressure equilibrium with the reservoir again is attained (referred to as the *relaxed* ideal condition). The conditions are further illustrated in Figure 5. The unequal equilibrium volumes in parts i and ii.b arise from the different salt activities.

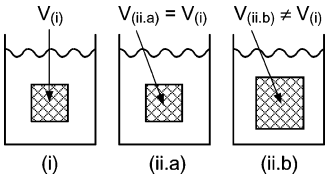

Figure 5. Illustration showing the gel (diamond-patterned area) in the reservoir of solvent for the nonideal condition labeled i, the unrelaxed ideal condition labeled ii.a, and the relaxed ideal condition labeled ii.b. Typically, $V_{(ii.b)} > V_{(i)}$.

At the nonideal condition, eqs 6, 7, 9, and 10 provide the following relation between c^{salt} and $c^{salt,res}$

$$(c_- + \nu_- c^{salt})^{\nu_-} (\nu_+ c^{salt})^{\nu_+} \exp(\mu^{ex}/k_B T) = (\nu_- c^{salt,res})^{\nu_-} (\nu_+ c^{salt,res})^{\nu_+} \exp(\mu^{ex,res}/k_B T) \quad (14a)$$

with the excess chemical potential in the gel equaling $\mu^{ex} = \nu_- \mu_-^{ex} + \nu_+ \mu_+^{ex}$ and similarly for $\mu^{ex,res}$ in the reservoir. We recall that c_- denotes the concentration of those counterions being present in a salt-free gel due to the network charges. For the case where $\nu_- = \nu_+$ (e.g., in a 1:1 or in a 2:2 electrolyte), eq 14a simplifies to

$$(c_- + c^{salt})(c^{salt}) \exp(\mu^{ex}/k_B T) = (c^{salt,res})^2 \exp(\mu^{ex,res}/k_B T) \quad (14b)$$

For the ideal condition, eq 14 reduces to

$$(c_{-0} + \nu_- c_0^{salt})^{\nu_-} (\nu_+ c_0^{salt})^{\nu_+} = (\nu_- c^{salt,res})^{\nu_-} (\nu_+ c^{salt,res})^{\nu_+} \quad (15a)$$

$$(c_{-0} + c_0^{salt})(c_0^{salt}) = (c^{salt,res})^2 \quad (15b)$$

where the subscript 0 indicates values at the ideal condition.

Computationally, at the unrelaxed ideal condition c_0^{salt} is simply evaluated from eq 15 with $c_{-0} = c_-$ for given values of $c^{salt,res}$. Under the relaxed ideal condition, the determination of c_0^{salt} is more complicated. First, the pressure equilibrium can be expressed as

$$P_{uncharged}(c_{network,0}) + P_{ion} = P_{ion}^{res} \quad (16)$$

where $P_{uncharged}(c_{network,0})$ is the osmotic pressure of the corresponding uncharged network, which depends on the concentration of network particles, $c_{network,0}$. This pressure contribution has to be determined from additional gel simulations of uncharged networks. Furthermore, P_{ion} and P_{ion}^{res} are the contributions to the osmotic pressure from the small ions in the gel and the reservoir, respectively, given by

$$P_{ion} = k_B T[c_{-0} + (\nu_- + \nu_+)c_0^{salt}] \quad (17)$$

$$P_{ion}^{res} = k_B T(\nu_- + \nu_+)c^{salt,res} \quad (18)$$

For a given value of $c^{\mathrm{salt,res}}$, the two unknown variables c_0^{salt} and $c_{\mathrm{network},0}$ can be determined self-consistently using the relation $c_{-0} \equiv |z_{\mathrm{bead}}|c_{\mathrm{network},0}/|z_{\mathrm{counerion}}|$ and eqs 15−18. The analysis using the unrelaxed ideal condition is technically easier as compared to the relaxed ideal condition and, as shown below, is still qualitatively correct.

The role of the electrostatic interaction and the hard-sphere excluded volume of the simple ions on the Donnan equilibrium can be assessed by comparing the salt concentration at the nonideal condition, c^{salt}, with the salt concentration at the ideal condition, c_0^{salt}. In the following, we will first examine the Donnan equilibrium of the reference system under the nonideal and unrelaxed ideal conditions and then the Donnan equilibrium of all the systems under both the nonideal and ideal conditions.

4.2.1. Reference System. The salt concentration in the gel at the nonideal and unrelaxed ideal conditions as a function of the salt concentration in the reservoir for the reference system is displayed in Figure 6a. It is observed that the salt concentration in the gel is smaller at unrelaxed ideal conditions throughout the full concentration range, even at the highest salt concentration $c^{\mathrm{salt,res}} = 360$ mM.

The ratio $c_0^{\mathrm{salt}}/c^{\mathrm{salt}}$ is shown in Figure 6b. The limit $c_0^{\mathrm{salt}}/c^{\mathrm{salt}} \to \exp[\mu^{\mathrm{ex}}/k_{\mathrm{B}}T\nu_+]$ as $c^{\mathrm{salt,res}} \to 0$, following from eqs 14 and 15, is also included in the plot. Under the ideal condition and at $c_- > 0$, eq 15 implies that $c_0^{\mathrm{salt}}/c^{\mathrm{salt,res}} < 1$ at all finite $c^{\mathrm{salt,res}}$. We observe that at the unrelaxed ideal condition the salt concentration in the gel is 3-fold underestimated at small salt concentrations and the ratio approaches ≈0.9 at the highest salt concentration investigated. The smaller salt concentration in the gel for the unrelaxed ideal condition ($c_0^{\mathrm{salt}} < c^{\mathrm{salt}}$) is related to the fact that $\exp[-(\mu^{\mathrm{ex}} - \mu^{\mathrm{ex,res}})/k_{\mathrm{B}}T] > 1$, or equivalently, the excess chemical potential of the salt is smaller in the gel than in the reservoir ($\mu^{\mathrm{ex}} < \mu^{\mathrm{ex,res}}$), cf. eqs 14b and 15b. Hence, this analysis shows that the excess part of the chemical potential strongly influences the salt concentration in the gel and as expected its effect is reduced at increasing salt concentration.

The excess chemical potential of the small ions in the reference gel at different salt concentrations in the reservoir is shown in Figure 6c, and we notice that both μ_-^{ex} and μ_+^{ex} are negative. From Figure 2b we see that $\mu_-^{\mathrm{ex,res}}$ and $\mu_+^{\mathrm{ex,res}}$ also are negative (except at very high salt concentrations). Hence, under the present conditions, nonideality reduces the chemical potential for both ionic species in the gel and in the reservoir. The reduction is larger in the gel, promoting an enhanced salt concentration in the gel as compared to the ideal condition.

In the reservoir, the excess chemical potential of counterions $\mu_-^{\mathrm{ex,res}}$ and co-ions $\mu_+^{\mathrm{ex,res}}$ are equal for symmetry reasons. However, in the gel they are generally unequal, $\mu_-^{\mathrm{ex}} \neq \mu_+^{\mathrm{ex}}$. Figure 6c shows that the excess chemical potential of the counterions is more negative than that of the co-ions, $\mu_-^{\mathrm{ex,res}} < \mu_+^{\mathrm{ex,res}}$. The difference is largest at zero salt concentration and reduces monotonically as salt is added. We propose the following simple rationale for this appearance (which will be supported by radial distribution functions presented below). Let us start by dividing the gel solution into two regions of different size (i) one smaller comprising the volume near the positively charged network and having a substantial positive electrostatic potential but of limited spatial extension and (ii) one larger further away from the network and with a negative electrostatic potential of smaller magnitude but of larger extension. Obviously, the former region is more favorable for the negatively charged counterions as compared to the latter region for the positively charged co-ions. As the salt concentration is increased, the difference in the magnitude of the electrostatic potentials between the two regions decreases, making the difference in excess chemical potential of cations and anions smaller.

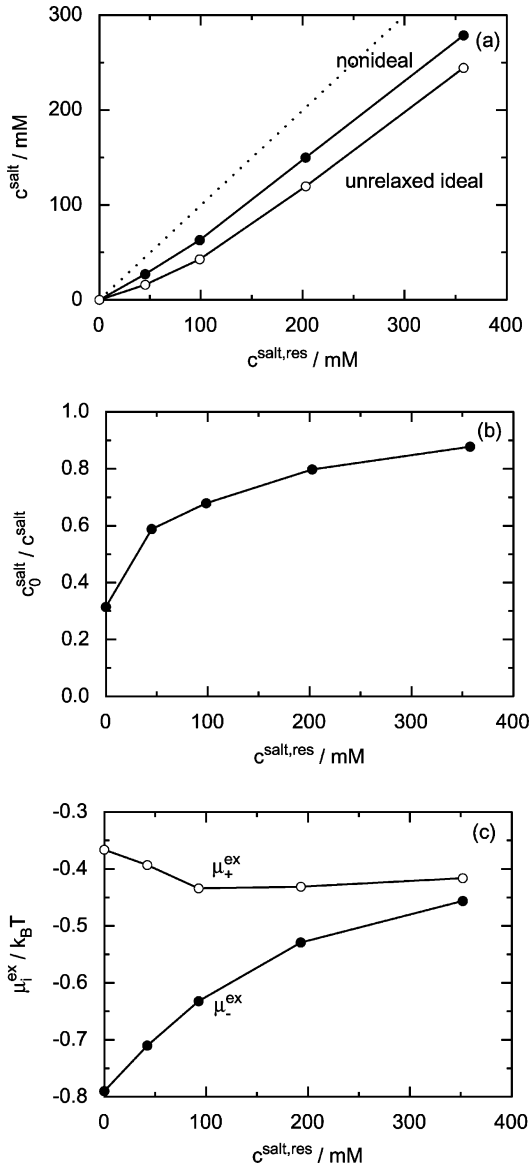

Figure 6. (a) Salt concentration in the gel for the nonideal (filled symbols) and unrelaxed ideal (open symbols) conditions, (b) ratio of the salt concentration in the gel for the unrelaxed ideal and nonideal conditions, and (c) reduced excess chemical potential for the negatively charged counterions (filled symbols) and the positively charged co-ions (open symbols) in the gel vs the salt concentration in the reservoir for the reference system. The lines are only guides to the eye. In part a, $c^{\mathrm{salt}} = c^{\mathrm{salt,res}}$ is indicated by a dotted line.

4.2.2. All Gel Systems. We will now examine the ratio $c^{\mathrm{salt}}/c^{\mathrm{salt,res}}$ for all systems and compare this ratio for the unrelaxed and relaxed ideal Donnan conditions with the nonideal condition. Figure 7 provides such results, and we notice that the values of the ratios for the nonideal (filled symbols) and unrelaxed (open sym-

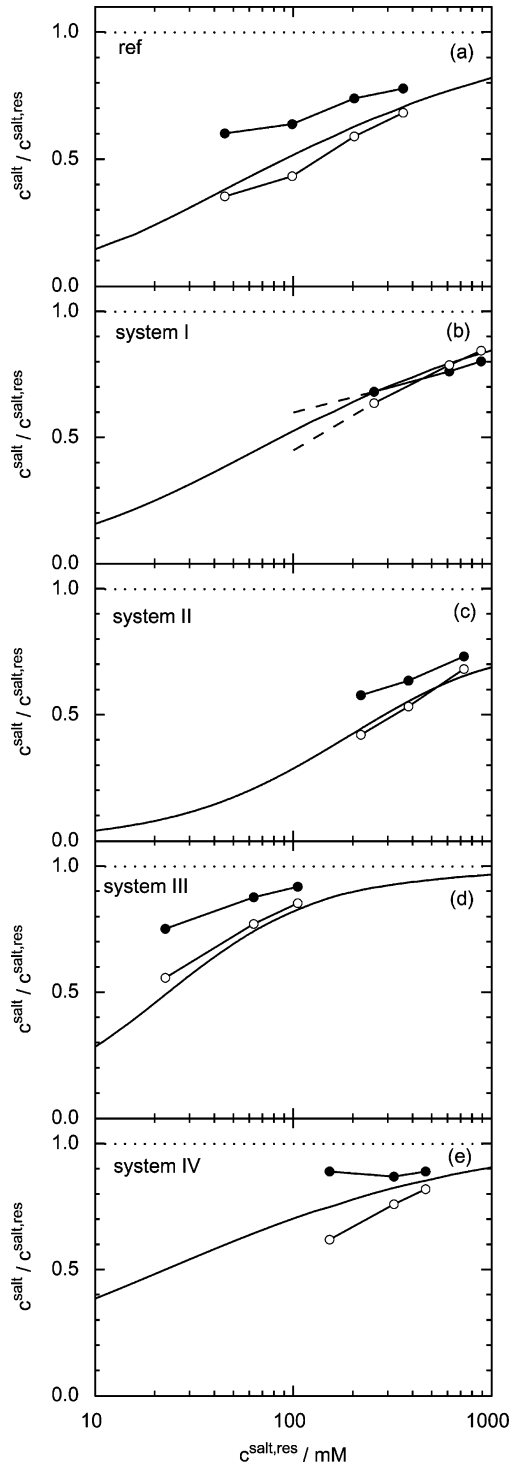

Figure 7. Ratio of the salt concentration in the gel and in the reservoir vs the salt concentration in the reservoir at the nonideal condition (filled symbols with connected lines), the unrelaxed ideal condition (open symbols with connected lines), and the relaxed ideal condition (solid curves) for (a) the reference system, (b) system I, (c) system II, (d) system III, and (e) system IV.

bols) ideal Donnan conditions are limited to the simulated $c^{salt,res}$ values, whereas the ratio under the relaxed ideal Donnan condition is continuous over the full concentration range (solid curve). The latter was calculated by using the osmotic pressure contribution from the network taken from interpolation of simulation data from uncharged gels.

Figure 7 confirms that the previous conclusions (i) $c_0^{salt} < c^{salt}$ and (ii) c_0^{salt}/c^{salt} increases as $c^{salt,res}$ is increased, made for the reference system, also apply to the other systems (with an possible exception at high salt concentration, further discussed below). Thus, we can with greater generality conclude that the excess chemical potential of the salt is smaller in the gel than in the reservoir. Moreover, in the limit $c^{salt,res} \to 0$, the unrelaxed ideal Donnan equilibrium condition underestimates the salt concentration in the gel by a factor of 2−6 (data not shown). By comparing the difference between the $c_0^{salt}/c^{salt,res}$ and $c^{salt}/c^{salt,res}$ curves at similar values of $c^{salt}/c^{salt,res}$ (e.g., ≈0.6), we conclude that the underestimation of the salt concentration in the gel reduces as the network linear charge density is decreased (reference system → system I), reduces as the cross-linking density is increased (reference system → system II), and reduces slightly as the chains are made stiffer (reference system → system III). The smaller difference between $c_0^{salt}/c^{salt,res}$ and $c^{salt}/c^{salt,res}$ at reduced linear charge density is expected due to the fact that the effect of nonideality should decrease as the electrostatic interaction is reduced.

We return to the observation $c_0^{salt} > c^{salt}$ and correspondingly $\mu^{ex} > \mu^{ex,res}$ for system I at $c^{salt,res} > 450$ mM (corresponding to $c_{network} + c_- + 2c^{salt} > 1$ M). At this particle density, we suggest that the hard-sphere packing effect becomes more important than the electrostatic interactions. We expect this to appear for the other systems as well at sufficiently high salt concentrations.

In addition, Figure 7 also shows that the difference between salt concentration in the gel under the unrelaxed and relaxed ideal Donnan conditions is generally small and less than the corresponding difference between the nonideal and ideal cases. However, the volume relaxation leads typically to a considerable increase of the gel volume, e.g., up 20% for the reference system and up to ≈100% for system IV. Nevertheless, the numerical simplicity of the unrelaxed ideal condition and its qualitatively accurate prediction of the salt concentration (as compared to the relaxed ideal condition) make it still useful.

To conclude this section, it is generally important to include the excess chemical potential of the ionic species to accurately predict the salt content in the gel, which is a prerequisite to obtain an accurate equilibrium volume. At high salt concentration this becomes however less important, primarily since the electrolyte conditions in the gel and in the reservoir become more similar, but at very high salt concentration the cancellation of the electrostatic and hard-sphere effects will also be of significance. Hence, the use of more accurate chemical potentials than provided by the EDH theory is necessary for an accurate prediction of equilibrium gel swelling in systems containing salt.

4.3. Gel Structure. 4.3.1. Snapshots. Figure 8 shows snapshots of the reference system in equilibrium with a reservoir with $c^{salt,res} = 45$ and 360 mM 1:1 electrolyte, corresponding to the smallest nonzero and highest salt concentration given in Table 3. At the lower salt concentration, the network still remains fairly expanded, however less so as compared to a gel in a salt-free solution (cf. Table 2 of ref 18 and Figure 8a). At the higher salt concentration, the chains are less expanded and the network is less regular. The space between the chains becomes much more occupied by the simple ions.

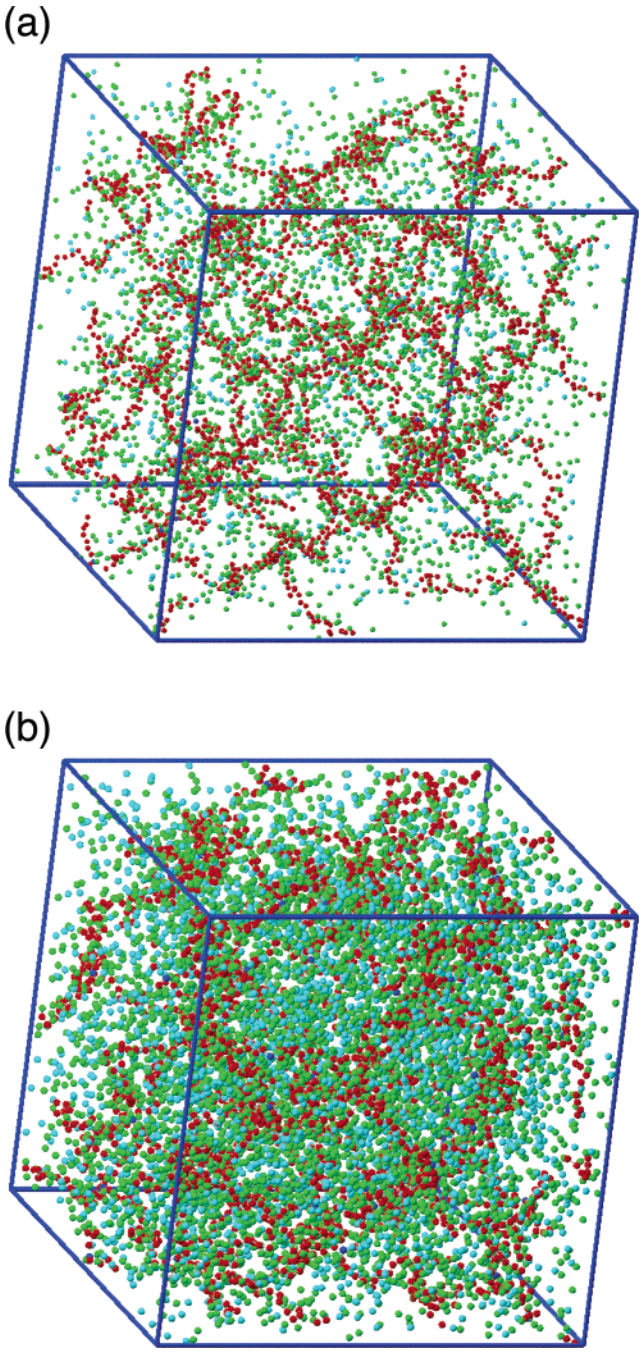

Figure 8. Snapshots of the reference system in equilibrium with a reservoir containing (a) 45 mM and (b) 358 mM 1:1 electrolyte displaying nodes (dark blue spheres), beads (red spheres), counterions (green spheres), and co-ions (light blue spheres) obtained from *NVT* simulations of systems containing eight unit cells. The lengths of the box sides are 34.0 and 25.0 nm, respectively, and the total numbers of particles are 6608 and 10496, respectively.

4.3.2. Radial Distribution Functions. The structure of the gels has been quantified by radial distribution functions (rdf's). The rdf $g_{ij}(r)$ denotes the relative density of particle j at distance r from particle i. At short separations, where particles would overlap, $g_{ij}(r) = 0$, whereas in a fluid at large separation, where the spatial correlations are lost, $g_{ij}(r) = 1$ by definition.

Figure 9 shows the 10 distinct rdf's at the two salt concentrations for which snapshots were given. The rdf's for the same system in equilibrium with a salt-free reservoir were given earlier.[18]

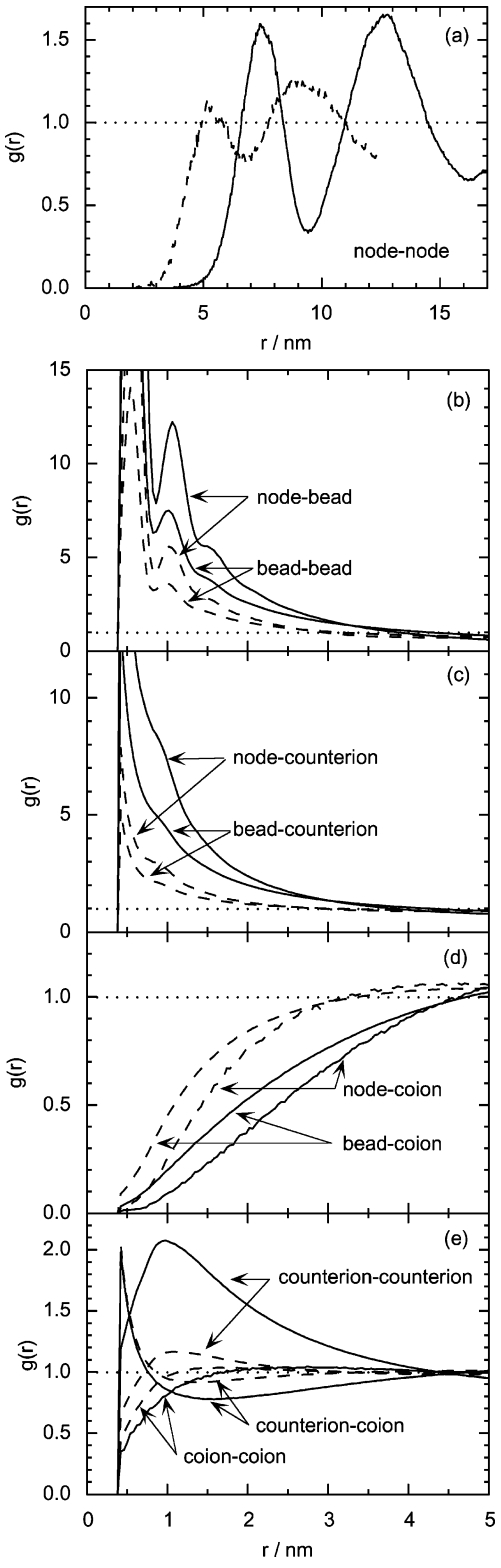

Figure 9. (a) Node−node, (b) node−bead and bead−bead, (c) node−counterion and bead−counterion, (d) node−co-ion and bead−co-ion, and (e) counterion−counterion, counterion−co-ion, and co-ion−co-ion radial distribution functions for the reference system in equilibrium with a reservoir containing (a) 45 mM (solid curves) and (b) 358 mM (dashed curves) 1:1 electrolyte obtained from *NVT* simulations of systems containing 8 unit cells. Note, the different scale of the abscissa in part a and parts b−e.

The node−node rdf's are given in Figure 9a. At the lower salt concentration (solid curve), two prominent peaks appear at $r \approx 7$ and 12.5 nm, respectively. As

previously argued,[18] the first one arises from the four nearest nodes linked to the central one by a single chain, whereas the second and broader peak involves 24 nodes, of which 12 are next nearest ones linked to the central one through two successive chains and the remaining 12 are linked to the central one by three successive chains and resides on the opposite side of the six-membered rings (see Figure 1). At the higher salt concentration (dashed curve), the peaks of the node−node rdfs are shifted to shorter r, and the separation of the characteristic node−node distances becomes less prominent.

Figure 9b shows that $g_{\text{node,bead}}(r)$ and $g_{\text{bead,bead}}(r)$ display large similarities: strongly peaked with an oscillatory behavior at short separation due to the chain connectivity and with a stronger amplitude for the one involving the node because each node is connected to four beads. The rdf's $g_{\text{node,counterion}}(r)$ and $g_{\text{bead,counterion}}(r)$ displayed in Figure 9c are similar and also strongly peaked at short separation. The accumulation of the counterions near network particles arises of course from their attractive electrostatic interactions and the higher relative density of counterions near a node as compared to a bead is an effect of the larger density of network particles near a node than near a bead. Figure 9d shows that also $g_{\text{node,co-ion}}(r)$ and $g_{\text{bead,co-ion}}(r)$ display similarities. The local density of co-ions within 3−5 nm is lower than the average co-ion density in the system. Moreover, the local density is lower near a node as compared to a bead, again an effect of the lattice topology. The deficiency of co-ions near the network originates from their repulsive electrostatic interaction. Hence, we conclude that $g_{\text{node},j}(r)$ and $g_{\text{bead},j}(r)$ with j = {bead, counterion, or co-ion} are pairwise similar, but with a more marked structure for $g_{\text{node},j}(r)$ as compared to $g_{\text{bead},j}(r)$. Moreover, parts b−d of Figure 9 show that as more salt is added and the equilibrium volume is reduced, the distribution of particles becomes more homogeneous. The reduction of the peak heights in parts b and c of Figure 9 is mainly an effect of a higher average concentration, and Figure 9d shows that the extension of the region near the network depleted of co-ions is reduced.

Finally, the three rdf's involving pairs of simple ions are provided in Figure 9e. A prominent feature is the large local density of counterions near a counterion, which is a consequence of them being attracted to the network. The $g_{\text{counterion,co-ion}}(r)$ displays a maximum at contact, but an extended region from 1 to 4 nm with a value below unity appears. The electrostatic attraction between counterions and co-ions leads to the formation of some pairs, but at larger distances the situation becomes more complex due to the locally heterogeneous solution. Last, $g_{\text{co-ion,co-ion}}(r)$ shows that co-ions are separated from each other at short separation. Again at the higher salt concentration, the features observed at the lower salt concentration become less prominent.

We now return to the difference excess chemical potential of the counterions and the co-ions. Parts c and d of Figure 9 confirmed that the environment of these small ions is widely different, the counterions being preferentially localized close to the charged network and the co-ions depleted from this region.

5. Comparison with the Flory−Rehner Theory

The Flory−Rehner (FR) theory[6,7] for uncharged gels augmented with the ideal Donnan equilibrium (referred to as the FRD theory) is still a very common ansatz to rationalize experimental swelling measurements of polyelectrolyte gels. For example, recently Okay and Sariisik[5] found satisfactory agreement with their experimental data of polyelectrolyte gels prepared from acrylamide and soldium acrylate monomers, provided that a linear charge density smaller than the actual one was assigned.

In the FRD theory, the osmotic pressure equilibrium between the polyelectrolyte gel and the reservoir containing a simple salt is expressed as

$$P_{\text{mix}} + P_{\text{eleastic}} + P_{\text{ion}} = P_{\text{ion}}^{\text{res}} \tag{19}$$

In eq 19, P_{mix} represents the contribution from mixing polymers and solvent and is given by

$$P_{\text{mix}} = -\frac{k_{\text{B}}T}{V_{\text{s}}}[\ln(1-\phi) + \phi + \chi\phi^2] \tag{20}$$

P_{eleastic} represents a purly enthalpic contribution from stretching of the chains and is given by

$$P_{\text{eleastic}} = -\frac{k_{\text{B}}T}{V_{\text{s}}N}\left(\phi^{1/3}\phi_0^{\,2/3} - \frac{\phi}{2}\right) \tag{21}$$

and P_{ion} and $P_{\text{ion}}^{\text{res}}$ are purely entropic contributions from the simple ions and are given by eqs 17 and 18, respectively. In eqs 20 and 21, ϕ denotes the network volume fraction in the gel, χ the polymer−solvent interaction parameter, N the number of segments in a chain connecting two successive nodes, ϕ_0 the network volume fraction in the gel after preparation, and V_{s} the molar volume of the solvent. The concentration of salt in the gel is described by the ideal Donnan equilibrium (and in our case with one of the salt components identical to the counterion of the polyelectrolyte gel given by eq 15). The concentration of counterions originated from the salt-free gel is given by $c_{-0} \equiv |z_{\text{bead}}|\phi/V_{\text{r}}|z_{\text{counerion}}|$, where V_{r} is the molar volume of a polymer segment.

In the following, we will compare the FRD theory with our simulated results for (i) uncharged gels, (ii) polyelectrolyte gels in equilibrium with a salt-free reservoir, and (iii) polyelectrolyte gels in equilibrium with salt-containing reservoirs.

The FRD theory possesses three parameters *not* appearing in our model. Here, we have adopted $\phi_0 = 0.04$, $V_{\text{s}} = 18$ mL/mol, and $V_{\text{r}} = 53$ mL/mol, values used by Okay and Sariisik[5] to model their experimental data. Moreover, $\chi = 0$ was assigned to emulate our hard-sphere interactions. In the FRD theory, the inverse network volume fraction, ϕ^{-1}, is often used to describe swelling of the gel, whereas in the primitive model the gel volume per network particle $v_{\text{eq}} = V_{\text{eq}}/N_{\text{network}}$ is an appropriate quantity. Unfortunately, there is no unambiguous relation between ϕ^{-1} and v_{eq} for the two approaches. Therefore, instead of discussing their absolute values, we will compare how ϕ^{-1} and v_{eq} depends on parameters describing the gel. In the following, ϕ^{-1} and v_{eq} will collectively be referred to as the specific volume of the network.

5.1. Uncharged Gels. Here, we will examine how the chain length of the network affects the gel volume. Table 4 provides the specific volumes of the uncharged reference system and uncharged system II, the latter only differing from the reference system by having 10 instead of 20 beads between connected nodes. Both the FR theory and the spring-bead model predict a smaller

Table 4. Swelling of Uncharged Gels and Polyelectrolyte Gels in Equilibrium with a Salt-Free Reservoir

gel system	FRD theory[a] ϕ^{-1} [b]	FRD theory[a] $\lvert\phi^{-1} - \phi_{ref}^{-1}\rvert/\phi_{ref}^{-1}$	this work v_{eq} (nm^3)[c]	this work $\lvert v_{eq} - v_{eq,ref}\rvert/v_{eq,ref}$
Uncharged Gel				
ref system	23.04	1	1.20	1
system II	17.68	0.23	0.842	0.30
Polyelectrolyte Gel				
ref system	462.9	1	25.9	1
system I	186.6	0.60	15.0	0.42
system II	189.4	0.59	7.50	0.71
system IV	183.8	0.60	3.70	0.85

[a] See text for values of parameters specific to the Flory–Rehner–Donnan theory. [b] Inverse of network volume fraction of the Flory–Rehner–Donnan theory. [c] Equilibrium volume per network particle $v_{eq} = V_{eq}/N_{network}$ of this work.

equilibrium volume for the shorter chain. The relative reductions of the specific volumes are 0.23 and 0.30, respectively, showing that the FR theory predicts a weaker sensitivity on the chain length. A possible reason could be the use of a Gaussian chain approximation in the FR theory, which becomes less appropriate for the relatively short chains.

5.2. Polyelectrolyte Gels with No Salt. In this case, the influence of the chain length of the network, valence of the network charges, and valence of the counterion charges on the specific gel volume will be considered. Table 4 also provides the specific volume of the reference system, system I, system II, and system IV for the case of the polyelectrolyte gels being in equilibrium with a salt-free reservoir.

First, a comparison of data for uncharged and charged gels given in Table 4 shows that the equilibrium volumes increase by more than 1 order of magnitude by charging up the network and the presence of counterions. Second, we conclude that as compared to the primitive model the FRD theory predicts: (A) a larger relative contraction of the gel as the linear charge density of the chains is reduced (0.60 vs 0.42 using the reference system and system I), (B) a smaller relative contraction as the chain length is reduced (0.59 vs 0.71 using the reference system and system II), and (C) smaller contraction as the monovalent counterions are replaced by divalent ones (0.60 vs 0.85 using the reference system and system IV). Conclusion A can be qualitatively explained by the fact that (i) the number of simple ions is less in system I and (ii) the contribution to the osmotic pressure of the simple ions is overestimated by the FRD theory. Conclusions B and C can be understood from the fact that electrostatic interactions become more pronounced, either from a denser network (system II) or by increasing the counterion valence (system IV). In both cases the *smaller relative* reduction of the specific volume as predicted by the FRD theory can be attributed to the increasing overestimation of the osmotic pressure contribution from the small ions. (Note, the main origin of the *reduction* of the specific volume as such is the shorter chain length and the smaller number of counterions, respectively.)

5.3. Polyelectrolyte Gels with Salt. In the last case, the deswelling of different gel systems upon the addition of salt will be examined. Figure 10a shows the inverse network volume fraction, ϕ^{-1}, from the FRD theory as a function of the salt concentration in the reservoir for different systems. As anticipated, the theory predicts a deswelling at increasing salt concentration. The relative deswelling is largest for the reference system, which also had the largest specific volume in equilibrium with a salt-free reservoir. Noticeable is the very similar inverse network volume fraction of system I, system II, and system IV at low salt concentration. The curves for system I and system IV nearly coincide due to the fact that (i) these systems contains the *same* number of simple ions per network particle (coming from the same $|z_{bead}|/|z_{counterion}|$ ratio) and (ii) the nonideal contributions due to direct electrostatic interactions to the osmotic pressure are neglected.

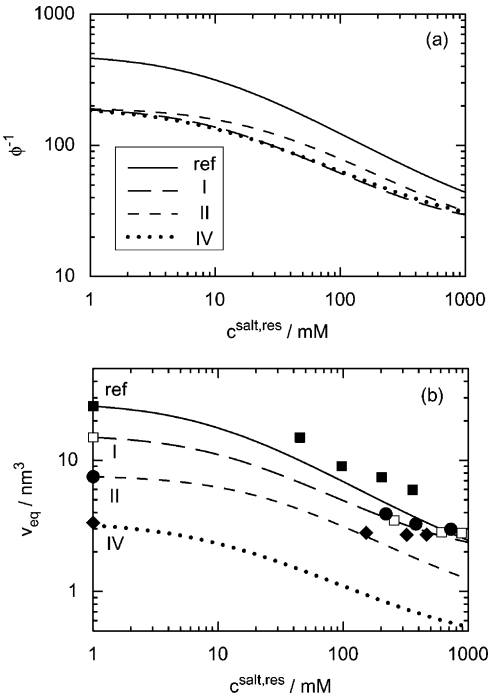

Figure 10. (a) Inverse network volume fraction ϕ^{-1} from the FRD theory and (b) equilibrium gel volume per network particle v_{eq} from the primitive model (symbols) and vertically rescaled inverse network volume fraction ϕ^{-1} from the FRD theory (curves) vs the salt concentration in the reservoir. In part b, the data from the primitive model at $c^{salt,res} = 1$ mM has been approximated with data for a salt-free reservoir, $c^{salt,res} = 0$ mM, and the data from the FRD theory are vertically rescaled (shifted in the logarithmic representation) such that each curve agrees with the corresponding curve from the primitive model at $c^{salt,res} = 1$ mM.

A comparison of the dependence of the salt concentration in the reservoir on the specific gel volumes for the two approaches is provided in Figure 10b. To facilitate such a comparison between the two approaches, the data from the FRD theory has vertically been *rescaled* for each system such that the specific volumes of the two approaches agree at the lowest salt concentration displayed. From the comparison, we conclude that the FRD theory predicts a stronger deswelling behavior for the reference system, system II, and system IV, but a similar deswelling prediction is noted for system I at increasing $c^{salt,res}$. Hence, the best prediction of the FRD theory is made for system I. This is reasonable since the ideal Donnan approximation should work best for the system with the weakest the electrostatic coupling. As the electrostatic coupling is increased, as in the reference system and in system II, the FRD theory overestimates the effect of salt. It can again be explained from the exaggeration of the ideal contribution from the simple ions to the osmotic pressure. This exaggeration is largest at low salt concentration and smaller at high salt concentration, where the errors in the gel and in the reservoir tend to cancel each other. For divalent

counterions the prediction of the FRD theory is worst. It predicts a greater deswelling than actually occurs and by 150 mM the overestimation is a factor 3 due to the neglect of the effect of electrostatic coupling.

Finally, we will return to the experimental results of Okay and Sariisik.[5] We propose that their need to use an effective network charge density smaller than the true one in the FRD theory to fit their experimental data originates from the accelerating exaggeration of the osmotic pressure from the presence of small ions at increasing chain linear charge density. An improved electroststic description would have reduced the need of invoking such an effective property.

6. Summary

On the basis of Monte Carlo simulations, properties of polyelectrolyte gels have been determined for gels with different (i) charge density, (ii) cross-linking density, (iii) chain flexibility, and (iv) counterion valence. The polyelectrolyte gel was described as composed of a defect-free three-dimensional network of a diamondlike topology and explicit simple ions. The network was formed by charged hard spheres connected by harmonic bonds, and the simple ions were represented by charged hard spheres.

Equilibrium volumes, salt contents, and structural aspects of the polyelectrolyte gels were determined for the gels being in equilibrium with a reservoir at different salt concentrations. Equilibrium conditions were established by requiring identical osmotic pressure and chemical potential of the salt in the gel and in the surrounding reservoir. The role of the electrostatic interactions has been addressed by examining the Donnan equilibrium under ideal conditions with and without volume relaxation. The predictions of the Flory−Rehner−Donnan theory and our results have also been made.

Our main findings and conclusions of this work are as follows:

(A) Polyelectrolyte gels undergo a deswelling as the salt concentration in the reservoir is increased, as also is experimentally well documented.

(B) At high salt concentration, the equilibrium volume of the gel is often still two to four times larger than the volume of the corresponding uncharged gel in equilibrium with a salt-free reservoir. Only polyelectrolyte gels with stiff chains attain equilibrium volumes of their corresponding uncharged gels.

(C) The salt concentration in a polyelectrolyte gel increases continuously as the salt concentration in the reservoir is increased. Nevertheless, the salt concentration remains substantially below that of the reservoir, even at nearly molar salt concentrations, due to a high concentration of network charges and associated counterions. Polyelectrolyte gels with stiff chains or divalent counterions constitute exceptions.

(D) Typically, the excess chemical potential of the salt is lower in the gel than in the reservoir, making the salt concentration in the gel larger as compared to the ideal condition. At high salt concentration, the Donnan equilibrium for ideal solutions becomes a better approximation, since the difference in the chemical potential of the salt in the polyelectrolyte gel and the reservoir becomes smaller. In the gel, the excess chemical potential of the counterions is more negative that that of the co-ions.

(E) The polyelectrolyte gel with stiff chains displays a smaller salt sensitivity, since, in the first place, the osmotic swelling only weakly increases the equilibrium volume. The low concentration of network charges and associated counterions makes it possible to attain nearly the same salt concentration in the gel as in the reservoir.

(F) The polyelectrolyte gel with divalent counterions is the least swollen gel, and its equilibrium volume is only weakly affected on an addition of a 2:1 salt.

(G) The inhomogeneous distribution of network particles and counterions in the gel at salt-free conditions becomes less inhomogeneous at increasing salt concentration.

(H) The predictions of the Flory−Rehner−Donnan theory are in most cases in qualitative agreement with our findings. However, substantial quantitative disagreements arise from an exaggerated contribution from the counterions to the osmotic pressure through a neglect of the difference in the chemical potential of the salt between the gel and the reservoir.

Acknowledgment. We are very grateful to Marcel van Eijk, Lennart Lindfors, and Lennart Picullel for generous discussions and valuable comments. This work was financed by the Centre for Amphiphilic Polymers from Renewable Resources (CAP).

References and Notes

(1) *Advances in Polymer Science*; Dusek, K., Ed.; Springer-Verlag: New York, 1993; Vols. 109 and 110.
(2) Katchalsky, A.; Michaeli, I. *J. Polym. Sci.* **1955**, *15*, 69.
(3) Ohimine, I.; Tanaka, T. *J. Chem. Phys.* **1982**, *77*, 5725.
(4) Ricka, J.; Tanaka, T. *Macromolecules* **1984**, *17*, 2916.
(5) Okay, O.; Sariisik, S. B. *Eur. Polym. J.* **2000**, *36*, 393.
(6) Flory, P. J.; Rehner, J. J. *J. Chem. Phys.* **1943**, *11*, 512.
(7) Flory, P. J.; Rehner, J. J. *J. Chem. Phys.* **1943**, *11*, 521.
(8) Wall, F. T. *J. Chem. Phys.* **1943**, *11*, 527.
(9) James, H. M.; Guth, E. *J. Chem. Phys.* **1943**, *11*, 455.
(10) Flory, P. J. *Principles of Polymer Chemistry*; Cornell University Press: Ithaca, NY, 1953.
(11) Donnan, F. G.; Guggenheim, E. A. *Z. Phys. Chem.* **1932**, *162*, 346.
(12) Overbeek, J. T. G. *Prog. Biophys. Biophys. Chem.* **1956**, *6*, 58.
(13) Khokhlov, A. R.; Starodubtzev, S. G.; Vasilevskaya, V. V. Conformational transitions in polymer gels: theory and experiment. In *Advances in Polymer Science*; Dusek, K., Ed.; Springer-Verlag: New York, 1993; Vol. 109; p 123.
(14) Allen, M. P.; Tildesley, D. J. *Computer Simulations of Liquids*; Oxford University Press: Oxford, England, 1987.
(15) *Monte Carlo and molecular dynamics simulations in polymer science*; Binder, K., Ed.; Oxford University Press: New York, 1995.
(16) Escobedo, F. A.; de Pablo, J. J. *Phys. Rep.* **1999**, *318*, 85.
(17) Schneider, S.; Linse, P. *Eur. Phys. J. E* **2002**, *8*, 457.
(18) Schneider, S.; Linse, P. *J. Phys. Chem. B* **2003**, *107*, 8030.
(19) Schneider, S.; Linse, P. *Macromolecules* **2004**, *37*, 3850.
(20) Yan, Q.; de Pablo, J. J. *Phys. Rev. Lett.* **2003**, *91*, 018301.
(21) Lu, Z.-Y.; Hentschke, R. *Phys. Rev. E.* **2003**, *67*, 061807.
(22) Akinchina, A.; Linse, P. *Macromolecules* **2002**, *35*, 5183.
(23) Metropolis, N. A.; Rosenbluth, A. W.; Rosenbluth, M. N.; Teller, A.; Teller, E. *J. Chem. Phys.* **1953**, *21*, 1087.
(24) Ewald, P. P. *Ann. Phys.* **1921**, *64*, 253.
(25) Lobaskin, V.; Linse, P. *J. Chem. Phys.* **1998**, *109*, 3530.
(26) Linse, P. MOLSIM; 3.4 ed.; Lund University: Lund, Sweden, 2003.
(27) Nymand, T. M.; Linse, P. *J. Chem. Phys.* **2000**, *112*, 6152.
(28) Widom, B. *J. Chem. Phys.* **1963**, *39*, 2808.
(29) Svensson, B. R.; Woodward, C. E. *Mol. Phys.* **1988**, *64*, 247.
(30) McQuarrie, D. A. *Statistical Mechanics*; Harper & Row: New York, 1973.

MA0486391